Appl. Phys. B 72, 743–748 (2001) / Digital Object Identifier (DOI) 10.1007/s003400100570

Applied Physics B
Lasers
and Optics

−70 dB optical carrier suppression by two-beam coupling in photorefractive media

D.Z. Anderson[1,*], V. Damiao[1], D. Popovic[2], Z. Popovic[2], S. Romisch[2], A. Sullivan[1]

[1] Department of Physics and JILA, University of Colorado, Boulder CO, 80309-0440, USA
[2] Deptartment of Electrical and Computer Engineering, University of Colorado, Boulder CO, 80309-0425, USA

Received: 29 November 2000/Revised version: 2 February 2001 /Published online: 27 April 2001 –

Abstract. Suppression of an optical carrier from an RF modulated laser beam of wavelength 532 nm is performed using two-beam coupling in photorefractive barium titanate. A theoretical analysis reveals that perfect suppression can be achieved at a specific modulation strength, which depends on the gain and intensity ratio between the two beams. The experiments achieve a maximum of -72.9 ± 2.4 dB carrier suppression at the theoretically ideal modulation strength, and -61.0 ± 2.4 dB for small modulation strengths.

PACS: 42.6.5-k; 42.65 Hw; 42.40.Kw

Optical modulators typically transmit some amount of optical carrier power along with the imposed sidebands. Phase modulators do so inherently, yet intensity modulators in practice also transmit carrier at a typical level of −30 dB below the input power. Acousto-optic modulators are nominally single sideband, yet typically −50 dB of the carrier power leaks into the output. Optical carrier energy is often unwanted, especially in certain optical communications and signal processing applications. Our work involves the optical processing of communications signals from an active antenna array in which the presence of an optical carrier introduces undesired spurious signal correlations [1].

Methods to suppress the carrier include both linear [2–5] and nonlinear optical techniques [6–11]. Frankel et al. [4] have reported better than −40 dB carrier suppression using a Sagnac fiber loop, and Loayssa et al. report a better than −55 dB result using a Brillouin-erbium fiber laser [9].

In optical communication links, for example, a balanced modulator scheme using a Mach–Zehnder interferometer can be used to convert phase-modulation into intensity modulation, as illustrated in Fig. 1. The modulators in each arm of the interferometer are driven in anti-phase. The recombining beamsplitter serves to subtract the two carriers while it adds the sideband energy. The optical path length difference between the two arms must be controlled in order to obtain the subtraction at the desired signal port. Good performance requires well-matched wavefronts, proper setting of the two beamsplitter splitting ratios, good balance between the two modulators and good servo-control to compensate for drifts in optical path lengths of the interferometer arms.

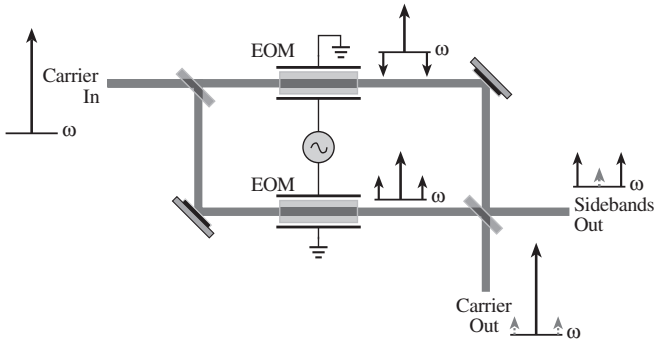

Fig. 1. A balanced Mach–Zehnder interferometer for suppressed carrier modulation subtracts the modulated signals from two electro-optic modulators (EOM) driven in antiphase

This work presents a demonstration of optical carrier suppression using two-beam coupling in photorefractive barium titanate. The scheme, shown in Fig. 2, is similar to an unbalanced version of the Mach–Zehnder modulator shown in

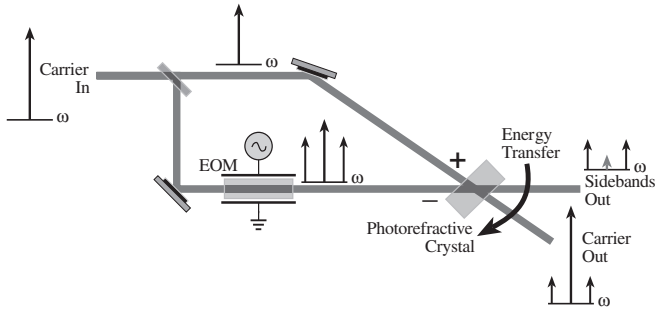

Fig. 2. A photorefractive interferometer adaptively subtracts most of the optical carrier from the modulated signal

*Corresponding author.
(Fax: +1-303/492-5504, E-mail: dana@jila.colorado.edu)

Fig. 1, except a photorefractive crystal replaces the recombining beamsplitter.

This change produces a system that is tolerant to wavefront mismatch and incoming intensity ratios, and automatically compensates for optical path length drifts of the two interferometer arms. The calculation presented below shows that two-beam coupling produces perfect carrier suppression for a certain fixed signal modulation depth – a result that is at first surprising. In practice, our experiments using a wavelength of 532 nm and photorefractive barium titanate achieve a maximum -72.9 ± 2.4 dB carrier suppression at a fixed modulation depth, and -61.0 ± 2.4 dB for small signal modulation.

1 Theory of optical carrier suppression

The analysis of carrier suppression considers two-beam coupling between two beams having different temporal characteristics. In our case, one beam is an unmodulated beam at the optical carrier wavelength, while the other is modulated rapidly compared with the photorefractive time constant. This problem has been analyzed extensively [12–34]. The primary focus has often been photorefractive-assisted homodyne or heterodyne detection, not carrier suppression. The work of Ringhofer et al. [34] highlights several characteristic features of two-beam coupling with modulated signals in a rather general framework. We investigate the theoretical carrier suppression performance using a matrix approach to photorefractive two-beam coupling [35]. The matrix approach provides good insight into the coupling dynamics, and in particular, provides a geometrical picture for the conditions of perfect carrier suppression.

Figure 3 establishes a context for the calculation. A signal-bearing beam is incident on the "minus" (−) port of the two-beam coupling interaction while an unmodulated carrier is incident on the "plus" (+) port. The interaction is arranged to transfer energy from the minus to the plus port. We have illustrated the modulated beam as a carrier with two sidebands, and the unmodulated beam as a simple carrier. In fact, the temporal structure of the "carrier" and "sidebands" can have practically any form provided the two remain uncorrelated on time scales corresponding to the photorefractive response time (on the order of 0.01 s to 1 s), and provided their bandwidths are not such that Bragg degeneracy is broken (on the order of tens of Gigahertz). In the experiment presented here, signals in the 100 MHz range are used.

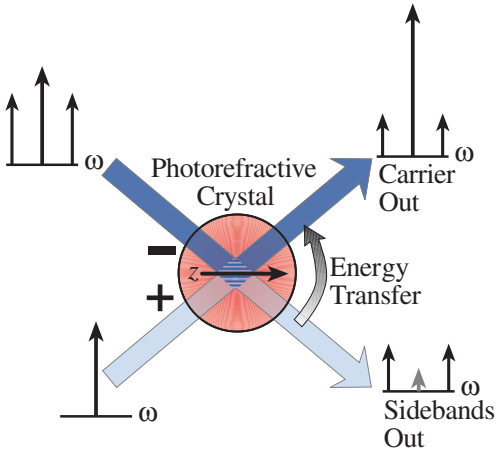

Fig. 3. Labeling and illustration of photorefractive two-beam coupling input and output

The matrix approach represents the optical fields in terms of fieldvectors; these fieldvectors evolve with distance z through the medium, as indicated in Fig. 3. We write the input ($z = 0$) carrier and signal fieldvectors as

$$\boldsymbol{e}_{\mathrm{c}}(0) = \begin{pmatrix} \sqrt{I_{\mathrm{c}_+}(0)} \\ \sqrt{I_{\mathrm{c}_-}(0)} \end{pmatrix}, \tag{1}$$

$$\boldsymbol{e}_{\mathrm{m}}(0) = \begin{pmatrix} 0 \\ \sqrt{I_{\mathrm{m}_-}(0)} \end{pmatrix}, \tag{2}$$

where $I_{\nu_\pm}$ the are intensities at the plus and minus ports. The two-beam coupling interaction serves to rotate these fieldvectors through an angle β via the rotation matrix:

$$T(z) = \begin{pmatrix} \cos\beta(z) & \sin\beta(z) \\ -\sin\beta(z) & \cos\beta(z) \end{pmatrix}. \tag{3}$$

Theoretically, perfect optical carrier suppression occurs when the rotation angle is such that the carrier energy is placed entirely at the plus port, that is, when the carrier fieldvector rotates by an amount:

$$\beta(z_{\mathrm{optimum}}) = \arctan\left(\frac{\sqrt{I_{\mathrm{c}_-}(0)}}{\sqrt{I_{\mathrm{c}_+}(0)}}\right). \tag{4}$$

The signal fieldvector rotates through the same angle, so some of its energy is lost to the plus port, yet its remaining energy at the minus port is uncontaminated by the optical carrier.

The rotation angle is found by first forming a "density matrix" [36] from the two fieldvectors:

$$\varrho = \begin{pmatrix} \varrho_{++} & \varrho_{+-} \\ \varrho_{-+} & \varrho_{--} \end{pmatrix} = \frac{1}{I_{\mathrm{c}} + I_{\mathrm{m}}}\left(\boldsymbol{e}_{\mathrm{c}} \times \boldsymbol{e}_{\mathrm{c}}^{\dagger} + \boldsymbol{e}_{\mathrm{m}} \times \boldsymbol{e}_{\mathrm{m}}^{\dagger}\right), \tag{5}$$

where I_{c} and I_{m} are the total carrier and signal intensities, $\dagger$ indicates complex-conjugate transpose (here simply transpose since the quantities are real) and the times symbol "$\times$" indicates outer product. The rotation angle can now be written in terms of density matrix quantities:

$$\beta(z) = \theta_0 - \theta(z), \tag{6}$$

where

$$\theta(z) = \arctan\left\{\exp\left[(-\Delta\lambda)z/2\right]\tan\theta_0\right\}, \tag{7}$$

and

$$\theta_0 = \arctan\left(\frac{\Delta\lambda + \varrho_{--} - \varrho_{++}}{2\varrho_{+-}}\right). \tag{8}$$

$\Delta\lambda$ is the difference between the two eigenvalues of the density matrix:

$$\Delta\lambda = \sqrt{1 + 4\left(|\varrho_{+-}|^2 - \varrho_{++}\varrho_{--}\right)}. \tag{9}$$

In (7) the interaction distance z is assumed to be measured in units of the photorefractive coupling constant, Γ^{-1}. The signal and carrier intensities at the output of the photorefractive medium having a given interaction length L, are obtained from the output fields:

$$\boldsymbol{e}_v(L) = T\,(L)\boldsymbol{e}_v(0)\,.$$

That there can be perfect carrier suppression is easily understood from a geometrical picture of the two-beam coupling interaction. The two vectors indicated in (1) and (2) are illustrated in Fig. 4a for $I_{c_+} = I_{c_-} = 1/\sqrt{2}$ and $I_{m_-} = 0.5$. The eigenvectors of the input density matrix, (5) , are also drawn. Their lengths are given by their respective eigenvalues. The eigenvector with the larger eigenvalue always lies in between the two input vectors. The action of the two-beam coupling serves to rotate the eigenvectors such that the one with the larger eigenvalue becomes aligned with the plus axis in the limit of the large interaction length, as shown in Fig. 4b. All the vectors rotate together; hence at some finite interaction distance the vector representing the optical carrier becomes aligned with the plus-axis, corresponding to its absence, or perfect suppression, from the minus port. For the carrier vector indicated in the figure the needed rotation angle is 45°, independent of the modulation strength. The interaction distance at which perfect suppression occurs, however, does depend on the relative intensities of the modulation and carrier. Since the interaction length is generally fixed in an experiment, perfect suppression occurs for a specific relationship among the carrier and signal intensities.

From an experimental viewpoint it is convenient to rewrite the quantities of interest in terms of two parameters. Let the splitting ratio be the ratio of the carrier intensity at the plus input port to the total intensity

$$c = \frac{I_{c_+}(0)}{I_{c_+}(0) + I_{c_-}(0) + I_{m_-}(0)}\,,$$

and let the modulation strength m be the intensity of the modulation sidebands relative to the total intensity at the input to the minus port:

$$m = \frac{I_{m_-}(0)}{I_{c_-}(0) + I_{m_-}(0)}\,.$$

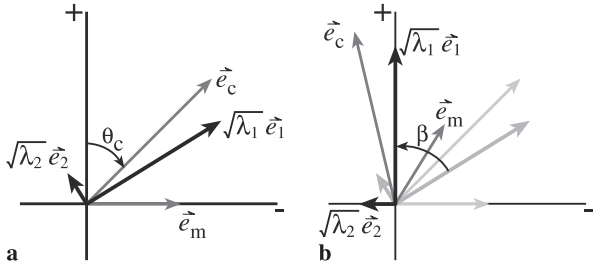

Fig. 4a,b. The geometrical picture of carrier suppression. **a** The carrier and modulated signal are represented by vectors $\vec{e}_c$ and $\vec{e}_m$, respectively. The density matrix eigenvectors and eigenvalues are represented by $\vec{e}_1$, λ_1 and $\vec{e}_2$, λ_2. **b** Two-beam coupling serves to rotate all vectors by the same angle. In the limit of large interaction distance the eigenvector with the largest eigenvalue is aligned along the plus (+) axis. At some point before that the carrier vector is entirely along the +-axis, indicating perfect carrier suppression

These two are convenient experimental quantities because c is set by the beamsplitter ratio at the input to the Mach–Zehnder interferometer (50/50 corresponds to $c = 0.5$), and m is then determined by the strength of the modulation. In terms of these two parameters:

$$\theta_c = \arctan\sqrt{\frac{(1-m)(1-c)}{c}}\,, \tag{10}$$

$$\Delta\lambda = \sqrt{1-4mc(1-c)}\,, \tag{11}$$

$$\theta_0 = \arctan\left[\frac{1-2c+\sqrt{1-4mc(1-c)}}{2\sqrt{(1-m)(1-c)c}}\right]. \tag{12}$$

Optimizing carrier suppression performance depends upon whether the modulation power is to be fixed or variable. When it is fixed, the optimum strategy is to satisfy (4) so that the theoretical perfect suppression is obtained. The required interaction length is given by combining (4), (6) and (7):

$$L = \frac{2}{\Delta\lambda}\ln\left[\frac{\tan(\theta_0)}{\tan(\theta_0-\theta_c)}\right]. \tag{13}$$

Analysis of this equation in conjunction with (10)–(12) shows that the interaction length required to obtain perfect suppression is minimized independent of the modulation strength m by choosing $c = 0.5$. Taking this value, one can then plot the required length dependence on modulation strength as in Fig. 5. The log–log plot nominally produces a straight line until the modulation strength approaches unity. At unit modulation strength there is no carrier energy on the modulated beam. An apparent paradox is worth comment: since there is no carrier, one might expect the required coupling strength ΓL to approach zero as $m \to 1$, not $\Gamma L = 4$, as it does in the plot. An arbitrarily small carrier power does, however, still require a finite coupling strength to be eliminated. The required coupling strength approaches a constant different from zero as the carrier power vanishes.

For applications for which the modulation strength is expected to vary, one is interested in the suppression performance over a range of signal strengths. The performance is assessed in Fig. 6 by determining the extent to which the modulation-to-carrier ratio is enhanced by the two-beam

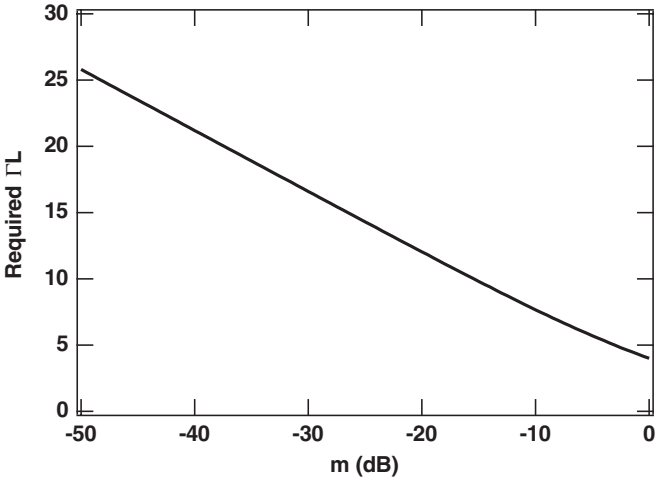

Fig. 5. Minimum required interaction length ΓL to achieve perfect carrier suppression

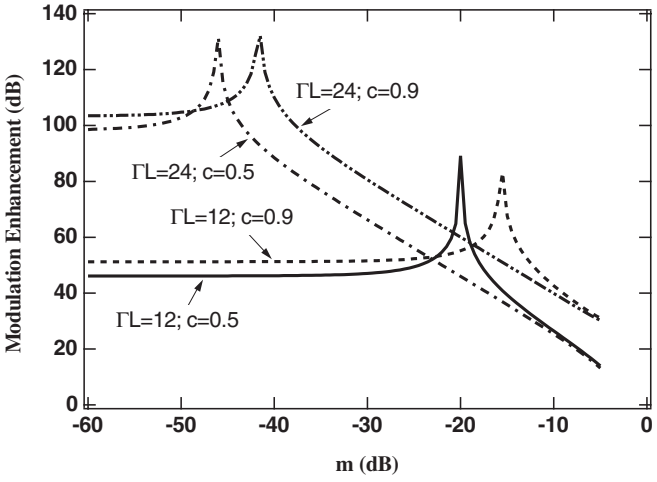

Fig. 6. Modulation enhancement due to photorefractive two-beam coupling. The *curves* give the modulation-to-carrier intensity ratio at the output versus the same ratio at the input for various values of the interaction length ΓL and the pump-to-total intensity ratio c

coupling interaction. The curves plot the signal-to-carrier intensity ratio at the output divided by the same ratio at the input, i.e.

$$R = \frac{I_{m\_}(L)/I_{c\_}(L)}{I_{m\_}(0)/I_{c\_}(0)} = \frac{I_{m\_}(L)/I_{c\_}(L)}{m/(1-m)} ,$$

versus m. We have chosen as a reference the solid curve representing $c = 0.5$ and $\Gamma L = 12$. For very small modulation strengths the enhancement factor is nominally constant at $R = 46$ dB. It then increases rapidly as the modulation corresponding to perfect suppression is approached so that $R \to \infty$. The enhancement falls thereafter. The remaining curves illustrate the effects of increasing the two adjustable parameters. Increasing the splitting ratio to $c = 0.9$ (dashed curve) moves the enhancement peak to larger modulation strength and increases the enhancement factor everywhere except around the peak of the reference curve. Doubling the gain factor to $\Gamma L = 24$ (dash–dot curve) dramatically increases the enhancement at low input modulation strengths until the reference curve begins to peak. The gain increase also moves the enhancement peak to a lower value of modulation strength. Unsurprisingly, increasing the splitting ratio to $c = 0.9$ at the higher gain factor (dash–double–dot) does much the same as it does for lower gain.

The set of plots leads to three design conclusions. First, if one is working with fixed modulation strength, the optimum design strategy simply sets the two-beam coupling gain to obtain theoretically perfect suppression. Second, if one is instead interested in good suppression performance over a range of modulation strengths, one obtains improved suppression at low modulation strength by increasing two-beam coupling gain but sacrifices some performance at larger modulation strengths (not to mention the increased cost of the crystal). Third, one can ameliorate the sacrifice by increasing the splitting ratio, but this reduces the absolute signal power, which is rarely desirable. We note that half of the signal power is lost to the plus port, and the photorefractive crystal additionally absorbs a portion of the signal energy (typically exp[−1/cm] for barium titanate in the visible region of the spectrum).

2 Experiment

We have demonstrated the carrier suppression concept using the experimental apparatus shown in Fig. 7. Laser light is supplied by a Coherent Inc. Verdi frequency-doubled diode-pumped Nd:YVO_4 laser ($\lambda = 532$ nm). About 4% of the beam is split off by a beamsplitter (BS) to provide a heterodyne reference. The major portion of the laser light is further divided by a half-wave plate/polarizing beamsplitter (PBS) combination arranged to provide nominally equal intensities at the photorefractive medium (i.e. $c = 0.5$). An RF signal at $f = 130$ MHz is imposed as phase-modulation sidebands onto the optical carrier using a Mg:$LiNbO_3$ elec-

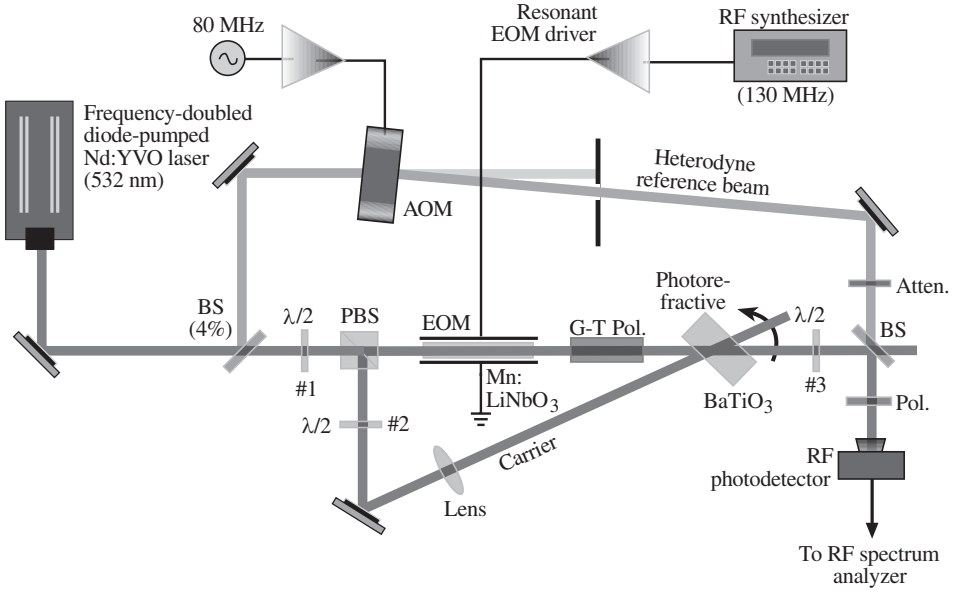

Fig. 7. Carrier suppression experimental apparatus

trooptic modulator (EOM). The modulator is followed by a Glan–Thompson calcite polarizer (G–T Pol.) having a specified extinction ratio of better than 1×10^{-6}. This polarizer eliminates the ordinary-polarized light that does not couple in the photorefractive medium, and which would otherwise leak through as unwanted optical carrier. The polarization of the unmodulated beam is rotated by a half-waveplate to provide the desired extraordinary polarization needed for two-beam coupling. We note that the polarization of this beam is not so critical as that of the modulated beam, so no additional polarizing element is employed. The photorefractive crystal is 0° cut and 6 mm along the c-axis direction. The angle between the modulated and unmodulated beams is about 20°, while the modulated beam is incident near Brewster's angle. A lens ensures that the carrier beam is larger than the modulated beam. The carrier-suppressed beam polarization is rotated to S-polarization with another half-wave plate.

The orientation of the Glan–Thompson polarizer is set by maximizing the contrast of the interferometer: With no modulation present, the output from the minus port of the photorefractive medium is nominally dark. Tapping on an interferometer mirror perturbs the relative optical path length and produces temporal fringes. The polarizer is rotated so that the peak-to-peak intensity observed with a photodetector and oscilloscope is maximized.

Experimentally, suppression is unambiguously characterized by the amount of carrier present at the minus port of the photorefractive medium. The degree of suppression is assessed using heterodyne detection: the heterodyne reference is frequency shifted from the carrier using an acousto-optic modulator operating at 80 MHz. This frequency-shifted beam is combined with the output beam from the photorefractive medium with a 50/50 beamsplitter and then detected. A sheet polarizer sitting immediately in front of the photodetector helps to eliminate residual scattered carrier light. The resulting signal is observed on an RF spectrum analyzer. The unsuppressed portion of the carrier appears as an 80 MHz signal, while the first-order sidebands appear at $f_{\pm} = |80 \pm 130|$ MHz. The acousto-optic modulator was itself observed to have carrier feedthrough at a level of -45 dB below its input energy. Since this feedthrough can obscure the desired measurement, the heterodyne reference beam is attenuated to be approximately 10^{-3} of the intensity of the modulated beam.

The electro-optic phase modulator imposes sidebands onto the optical carrier with the modulation strength given by $m = 1 - J_0^2(\alpha)$, where J_0 is the zero-order Bessel function and its argument α is the modulation index. The modulation index is proportional to the drive voltage to the modulator, $\alpha = \kappa V$, and thus provides a convenient means of finding κ to calibrate the modulation strength. In particular, $J_0(2.4048) \cong 0$, so $m(\kappa V = 2.4048) \cong 1$.

Figure 8 presents the experimental data of the optical carrier power versus modulation index. The vertical scale indicates optical carrier power, where 0 dB represents no carrier suppression. The dip at a modulation index of $\alpha = 2.405$ is simply due to the zero of the zero-order Bessel function corresponding to no carrier present at the minus port. Superimposed on the data is a calculated fit from the theory. As the apparent performance of the system depends on how one does the fitting, some remarks are in order.

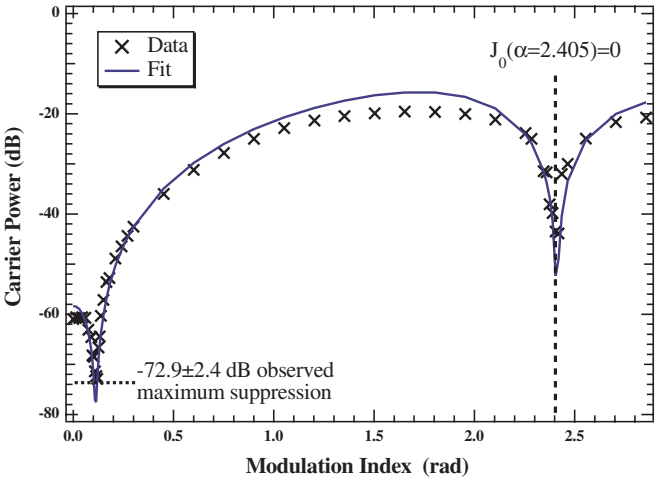

Fig. 8. Carrier power versus modulation index. 0 dB corresponds to an unsuppressed carrier

Carrier suppression is a highly nonlinear function of the modulation index α:

$$10 \log \left[\frac{I_{c_-}(L)}{I_{c_-}(0)} \right] = 20 \log \left[\cos \beta(\alpha) - \sqrt{\frac{c}{(1-c)(1-m(\alpha))}} \sin \beta(\alpha) \right],$$

where β is given by (6)–(9) and α itself has a nonlinear dependence on the drive voltage as the zero-order Bessel function. In short, the suppression data has an unpleasant functional form for curve fitting. To the above expression we also added a constant term δ representing the finite obtainable suppression due to instrumentation noise. The fit parameters are the two-beam coupling gain ΓL, the beam splitting intensity ratio c, the 0 dB suppression reference level, the calibration constant κ of the modulator and the noise level δ. The latter two were kept fixed at the experimentally observed values.

The fit estimates a two-beam coupling gain $\Gamma L = 13.05 \pm 0.16$. The fit also provides the 0-dB suppression reference level for the data shown in Fig. 8. For modulation indexes below about $\alpha = 0.05$ the observed carrier suppression is constant at -60.8 ± 2.4 dB, and the observed maximum suppression is -72.9 ± 2.4 dB at $\alpha = 0.12$. The best fit estimates the plus-to-minus intensity ratio to be $c = 0.60 \pm 0.05$, rather than the nominal $c = 0.5$ arranged in the experiment. This 20% deviation lies within a 95% confidence range. It is a large deviation, yet the theory assumes plane waves whereas the actual beams are Gaussian and, furthermore, the beam sizes are poorly determined. A fit with the splitting ratio parameter fixed to $c = 0.50$ gives a maximum suppression of -69.4 ± 1.0 dB.

As Fig. 8 suggests there are systematic effects at play, and the outcome of the fit routine depends on whether one chooses to bias the fit to data at high or low values of modulation indexes, in some other way, or not at all. The values and uncertainties quoted above reflect the "best fit". One can bias the fit to the data at low modulation strengths so the curve closely matches the data at zero modulation strength. This leads to more conservative estimates of the suppression performance than an unweighted fit, namely the maximum suppression becomes -70.0 ± 2.4 dB.

The suppression performance was also checked by measuring the carrier power with the unmodulated beam of the plus-port blocked. This provides an underestimate of the carrier suppression because the fanning of the modulated beam that occurs in the absence of the carrier reference beam also reduces the amount of carrier (and signal). By this method we would conclude that the carrier is suppressed by -52 dB for modulation indexes below 0.05 and by a maximum of -64.5 dB. If in the curve fitting one fixes the reference level to be consistent with blocked-carrier measurement, the resulting fit is comparatively poor, however. The 8 dB or so difference with the best fit is consistent with the blocked-carrier method being a conservative one.

Near the point of maximum carrier suppression the instrumentation noise floor combined with the carrier leakage of the acousto-optic modulator limited the measurements. -70 dB suppression corresponds to an interferometric stability of better than $\Delta\lambda/\lambda \approx 10^{-4}$. Hence the suppression performance was also limited by acoustic and vibration perturbations to the optical system.

3 Discussion

We have shown that optical carrier suppression can be achieved with a photorefractive two-beam coupling interferometer. At low signal strengths the suppression is primarily dependent on the gain of the two-beam coupling interaction. The theoretical analysis reveals that perfect suppression can be achieved for a specific modulation strength that depends on the two-beam coupling gain and the relative intensities of the two beams incident on the photorefractive medium. The scheme inherently loses about 3 dB of the signal to the plus port of the medium, and there are also reflection and absorption losses due to the medium that typically give another 1 dB to 3 dB overall insertion loss. Our experiments attained carrier suppression of -60.8 ± 2.4 dB at low modulation strengths and a maximum of -72.9 ± 2.4 dB. In terms of raw carrier suppression performance this is comparable to, and better than (respectively), the best results reported in the literature of which we are aware [9].

The experiments were carried out at a wavelength of 532 nm. Barium titanate and many other photorefractive materials have an inherently broad spectral response. It should be possible to perform carrier suppression anywhere throughout the visible spectrum and into the near-infrared with performance comparable to what we have reported here. In the infrared, however, and in particular at the common 1.5 μm or 1.3 μm communication wavelengths, such performance is probably not possible with currently available photorefractive materials.

Acknowledgements. We gratefully acknowledge the support provided by the National Science Foundation, through Grant No. PHY-9512150, and Grant No. ECS-9979355, and the Office of Naval Research and the Office of the Secretary of Defense through the MURI program, Grant No. N00014-97-1-1006.

References

1. D.Z. Anderson, V. Damiao, E. Fotheringham, D. Popovic, S. Romisch, A. Sullivan, Z. Popovich: *Optically Smart Active Antenna Arrays.* In IEEE Int. Microwave Symp. 2000, Boston, MA, USA
2. R.D. Esman, K.J. Williams: IEEE Photonics Technol. Lett. **7**, 218 (1995)
3. R. Montgomery, R. Desalvo: IEEE Photonics Technol. Lett. **7**, 434 (1995)
4. M.Y. Frankel, R.D. Esman: J. Lightwave Technol. **16**, 859 (1998)
5. A.C. Lindsay: IEEE Trans. Microwave Theory Techn. **47**, 1194 (1999)
6. K.J. Williams, R.D. Esman: Electron. Lett. **30**, 1965 (1994)
7. F.S. Yang, M.E. Marhic, L.G. Kazovsky: Electron. Lett. **34**, 2148 (1998)
8. A. Loayssa, D. Benito, M.J. Garde: Opt. Lett. **25**, 1234 (2000)
9. A. Loayssa, D. Benito, M.J. Garde: Opt. Lett. **25**, 197 (2000)
10. S. Tonda-Goldstein, D. Dolfi, J.P. Huignard, G. Charlet, J. Chazelas: Electron. Lett. **36**, 944 (2000)
11. F.S. Yang, M.E. Marhic, L.G. Kazovsky: J. Lightwave Technol. **18**, 512 (2000)
12. J.P. Monchalin: Rev. Sci. Instrum. **56**, 543 (1985)
13. G.H. Demonchenault, J.P. Huignard: J. Appl. Phys. **63**, 624 (1988)
14. F.M. Davidson, L. Boutsikaris: Opt. Eng. **29**, 369 (1990)
15. F. Davidson, C. Field, X. Sun: IEEE Photonics Technol. Lett. **4**, 1295 (1992)
16. S. Breugnot, M. Defour, H. Rajbenbach, J.P. Huignard: Opt. Commun. **104**, 118 (1993)
17. F. Davidson, C.T. Field: IEEE Photonics Technol. Lett. **5**, 1238 (1993)
18. C.T. Field, F.M. Davidson: Appl. Opt. **32**, 5285 (1993)
19. J. Khoury, V. Ryan, M. Croningolomb, C. Woods: J. Opt. Soc. Am. B: Opt. Phys. **10**, 72 (1993)
20. F.M. Davidson, C.T. Field: J. Lightwave Technol. **12**, 1207 (1994)
21. C.T. Field, F. Davidson: Opt. Lett. **19**, 78 (1994)
22. J. Khoury, M. Croningolomb, C. Woods: Appl. Opt. **33**, 5390 (1994)
23. P. Delaye, A. Blouin, D. Drolet, J.P. Monchalin: Appl. Phys. Lett. **67**, 3251 (1995)
24. S.P. Bian, J. Frejlich: J. Modern Opt. **43**, 1185 (1996)
25. B.F. Pouet, R.K. Ing, S. Krishnaswamy, D. Royer: Appl. Phys. Lett. **69**, 3782 (1996)
26. L.A. de Montmorillon, P. Delaye, J.C. Launay, G. Roosen: J. Appl. Phys. **82**, 5913 (1997)
27. P. Delaye, L. Frey, A. Mugnier, G. Roosen: Opt. Commun. **139**, 148 (1997)
28. Y. Li, Z.X. Zhou, X.D. Sun, Y.Y. Yiang, K.B. Xu: Opt. Commun. **136**, 160 (1997)
29. T.R. Moore, R.L. Blair, A.J. Megofna, M.P. Rieger, B.L. Shoop: Appl. Opt. **37**, 5176 (1998)
30. D. Statman, J.C. Lombardi: J. Nonlinear Opt. Phys. Mat. **7**, 47 (1998)
31. P. Delaye, A. Blouin, D. Drolet, J.P. Monchalin, L.A. de Montmorillon, G. Roosen: Appl. Phys. Lett. **74**, 3087 (1999)
32. R.J. Dewhurst, Q. Shan: Meas. Sci. Technol. **10**, R139 (1999)
33. Z.X. Zhou, Y. Li, Y.Y. Yiang, C.F. Hou, X.D. Sun: Opt. Commun. **168**, 409 (1999)
34. K.H. Ringhofer, V.P. Kamenov, B.I. Sturmann, A. Chernykh: Phys. Rev. E **61**, 2029 (2000)
35. D.Z. Anderson, R.W. Brockett, N. Nuttall: Phys. Rev. Lett. **82**, 1418 (1999)
36. L.I. Schiff: *Quantum Mechanics.* Int. Ser. in Pure and Applied Physics, ed. by L.I. Schiff (McGraw-Hill, New York 1968) p. 544